The Photosynthetic Bacterial Reaction
Center: Structure and Dynamics,pp.369-377
(Nato ASI Series A: Life Sciences,149,
Plenum Publ. Corp.,New York,1988)

ELECTROSTATIC CONTROL OF ELECTRON TRANSFER IN THE PHOTOSYNTHETIC REACTION CENTER OF *Rhodopseudomonas viridis*

H. Treutlein *, K. Schulten *, C. Niedermeier *,
J. Deisenhofer +, H. Michel +, D. DeVault †

* Physik-Department, Technische Universität München, D-8046 Garching, FRG
+ Max-Planck-Institut für Biochemie, D-8033 Martinsried, FRG
† Dept. of Physiology and Biophysics, Univ. of Illinois, Urbana, IL 61801, USA

ABSTRACT

We have investigated electrostatic properties of the photosynthetic reaction center of *Rhodopseudomonas viridis* , the molecular structure of which has been solved recently by X-ray crystallographic analysis[1,2]. Our calculations involved both time-averaged electrostatic properties as can be obtained from the static X-ray structure of the protein as well as fluctuating and time-varying electrostatic properties due to thermal motion of the reaction center and structural rearrangment after electron transfer. The latter properties were derived from a molecular dynamics simulation[3].

1. INTRODUCTION

The electrostatic interaction is one of the most important contributions to the total molecular energy and seems to play a major role for structure and function of biological macromolecules[4,5]. Such role of electrostatic interactions can be expected, in particular, for the photosynthetic reaction center which functions as a biological photodiode separating electron and hole charges.

Although Coulomb's law looks rather simple, the calculation of electrostatics inside and outside of macromolecules remains a problem to this day. The difficulty arises because of the the long range of electrostatic interactions and, hence, the large number of atom-pairs carrying fractional charges which contribute. The Coulomb interaction can be evaluated for all these pairs only for the equilibrium structure. Results of such calulation are presented in Sect. 2. Fluctuating and time-varying electrostatic properties originating from thermal motions and structural rearrangements can be described only in an approximate way. In fact, molecular dynamics simulations account only for Coulomb forces between atoms with distances less than a certain cutoff, modifying the force to keep resulting artifical effects small[6].

We have evaluated fluctuating and time-varying electrostatic properties on the basis of a molecular dynamics simulation also presented in these proceedings[3]. The results are presented in Sect. 3. The simulation started from an X-ray structure at 3 Å resolution[1,2]. We investigated the dynamical properties and the response of the protein to the primary electron transfer step simulated by re-charging the apropriate

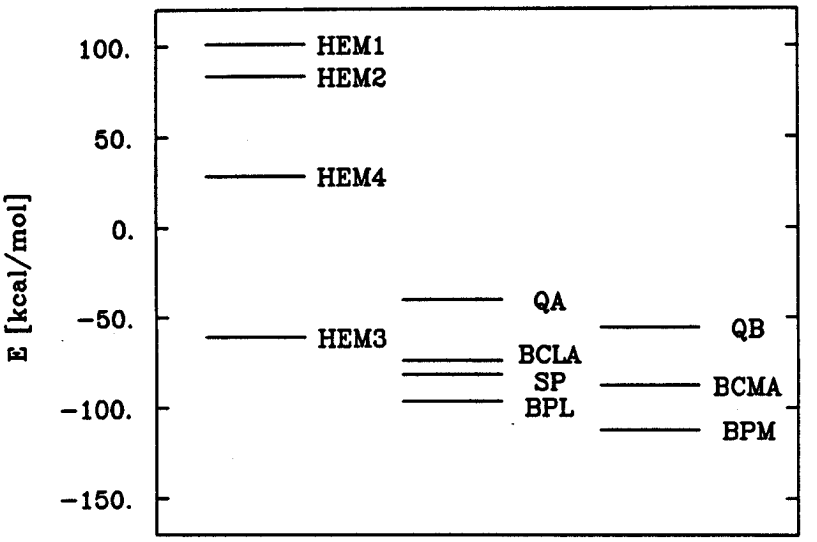

Fig. 1. Mean electrostatic potential levels of reaction center chromophores with neutral special pair and neutral non-heme iron site. The calculations are based on the X-ray structure.

chromophores. The simulation had been carried out in two steps: First, uncharged chromophores were assumed for the dynamics and the reaction center was analyzed in the state before electron transfer. Second, the *special pair* was positively and the bacteriopheophytine of the functional branch (BPL) negatively charged to analyze the state after primary electron transfer.

2. Mean electrostatic potentials of chromophores

As a first step in our investigation we have studied the mean electrostatic potential on the chromophores, i.e. the work done on an electron charge $(-e)$ brought from infinity to the site of the reaction center chromophores. For this purpose we included Coulomb interactions with fractional charges on all reaction center atoms including hydrogens. The fractional charges were those given in the **CHARMM** data base except for the charge distributions of glutamate M232 (see below), the four histidines ligated to the non-heme iron FE1 and the non-heme chromophores. The charge distributions for those residues and chromophores had been obtained by **MNDO** calculations.

The mean electrostatic potentials of the individual chromophores were obtained in two steps:

1. A negative test charge $(-e)$ was brough from infinity (∞) to the central chromophore (tetrapyrol rings and quinone, menaquinone rings) atoms at positions $\vec{r}$ and the energy difference $\Delta V(\vec{r}) = V(\vec{r}) - V(\infty)$ was determined by summing the Coulomb contributions of all charges inside the reaction center, with the exception of the charges on the same tetrapyrol or quinone rings. The influence of the latter should be attributed to the redox energy of a chromophore. In case of the special pair (SP) the Coulomb interactions between the two tetrapyrol moieties were also not counted.
2. The mean potential was then evaluated by averaging over the potential differences $\Delta V(\vec{r})$ of all atoms belonging to the ring systems of the individual chromophores.

We considered four different situations concerning the net charges of the spe-

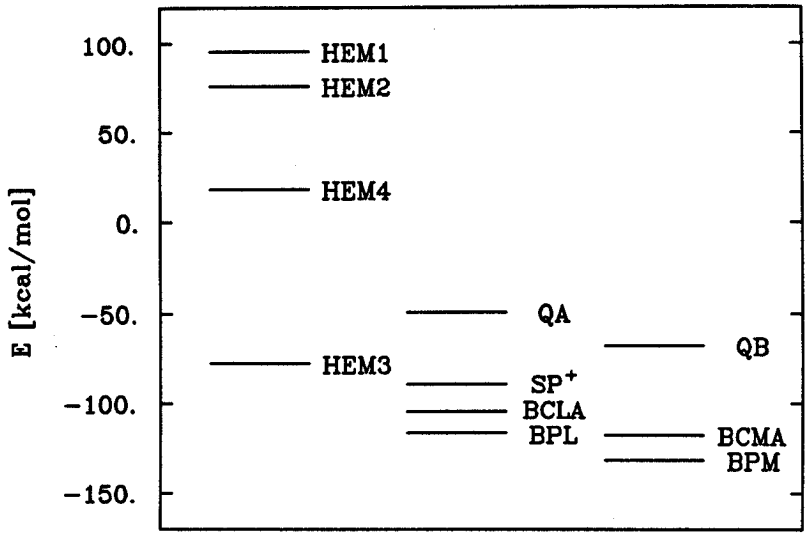

Fig. 2. Mean electrostatic potential levels of reaction center chromophores with positively charged special pair and neutral non-heme iron site.

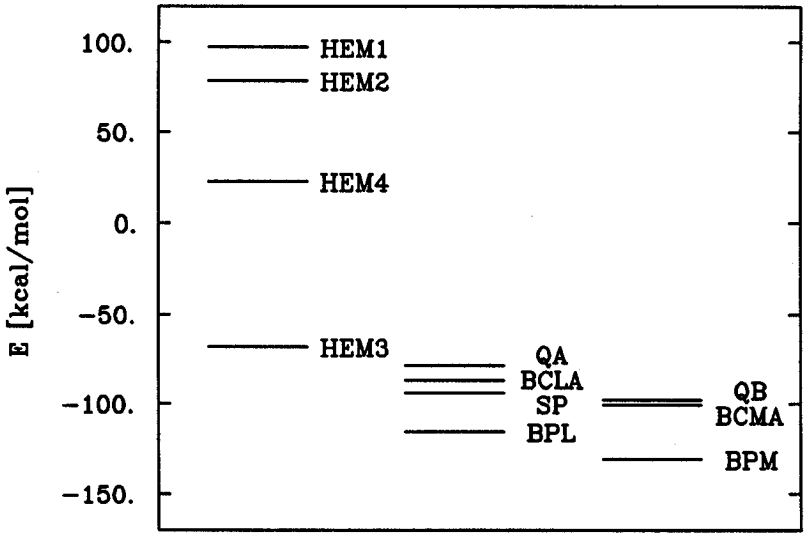

Fig. 3. Mean electrostatic potential levels of reaction center chromophores with neutral special pair and positively charged non-heme iron site.

cial pair and the non-heme iron site FE1: (i) SP-FE1, (ii) SP^+-FE1, (iii) SP-$FE1^+$, (iv) SP^+-$FE1^+$. The different charge states represented in the energy level diagrams Fig. 1–4 were chosen for the following reasons: In case of the special pair the transferred electron actually 'sees' a positively charged special pair (SP^+). Hence, in a description of primary and secondary transfer in terms of electrostatic potentials the *special pair* should be positively charged. Just in order to estimate the influence of localized charges on the chromophore energy levels we have also investigated the case of a neutral special pair. As for the non-heme iron site it is not apparent what the net charge should be. For this reason we investigated both the case of a neutral and of a positively charged ($+e$) state.

Our method of determining energy levels (mean electrostatic potentials) bear

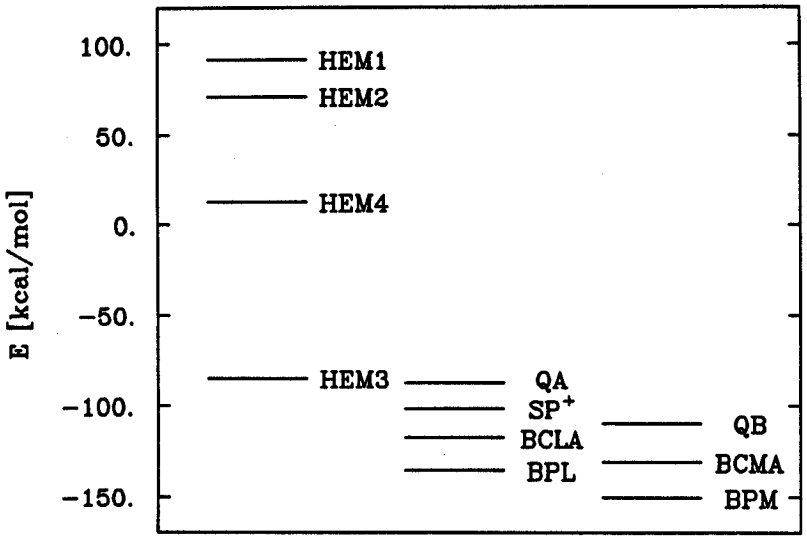

Fig. 4. Mean electrostatic potential levels of reaction center chromophores with positively charged special pair and positively charged non-heme iron site.

some obvious deficiencies. First, we did not include the water and membrane fraction surrounding the reaction center which will exert dielectric screening also on charges inside the reaction center. Also we did not include dielectric screening inside the reaction center due to the infinite frequency dielectric constant (optical density). Second, the H-unit of the reaction center complex carries six net negative charges ($-6e$) which are located at the protein surface and, therefore, can be neutralized partially by H^+ in the water fraction. Third, we cannot judge the accuracy of the (**CHARMM** and **MNDO**) charge distributions assumed in our calculations. Furthermore, there has been some degree of arbitrariness in assigning a protonated state to glutamate L104. Also we assumed that the hemes possess the same charge distributions as in myoglobin, i.e. there were two negatively charged carboxyl groups attached to each heme ring. These charges might explain the high electrostatic potential of the hemes in Fig. 1–4. However, if these carboxyl charges are neutralized, the heme potentials are shifted to values which are unacceptably low. The negative charges of carboxyl groups were also present on the chlorophylls and pheophytins, however, in this case the rings did not carry a net charge except in case (ii) and (iv) defined above.

In our evaluation of energy levels we assumed equal contributions of electrostatic potentials by all ring atoms. This assumption could be replaced by an atom-dependent weighting with weights determined through **MNDO** calculations.

We want to discuss now the energy level diagrams which resulted from our calculations for the charge situations (i) – (iv). The first observation is that the relative ordering of the energy levels is the same in all situations except for the SP–BCLA ordering which is reversed upon charging the special pair (SP $\rightarrow$ SP$^+$). The heme energy levels are found to be more positive than those for the other chromophores in accordance with the function of the hemes as hole carriers. However, the heme energies are spread over a very broad energy range. We attribute this to a neglect of the water fraction surrounding the cytochrome unit and contributing an effective dielectric screening. The energy levels of the M (non-functional) branch chromophores QB, BCMA, BPM are more negative than their L (functional) branch counterparts. This is opposite to the findings of Yeates et al.[7] for the *Rps. sphaeroides* reaction center which also accounted for the effect of a heterogeneous dielectric (water–membrane) surrounding.

The lower position of the energy levels of the non-functional chromophores relative to the levels of the respective functional chromophores does not necessarily imply

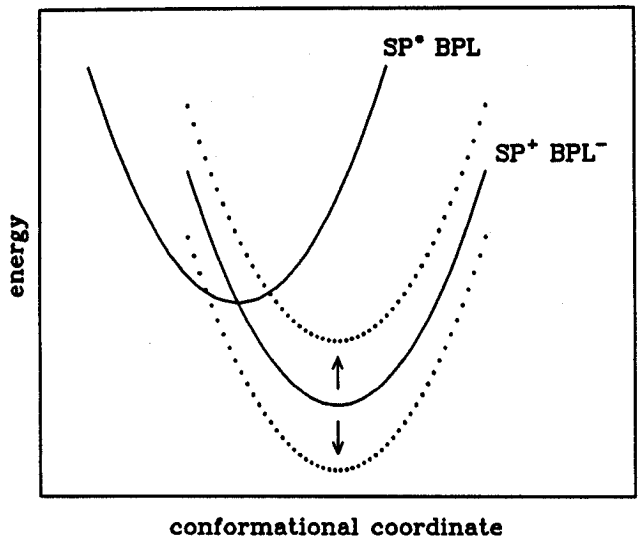

Fig. 5. Nuclear potential energies of neutral (SP^*-BPL) and charged (SP^+-BPL^-) states depending on a generalized conformational coordinate. Solid lines denote an optimum crossing. Dotted lines show hypothetically shifted potential functions, which result in a thermal activation barrier.

a more favourable, i.e. faster, route for electron transfer along this branch relative to the functional branch. Since observations show that primary electron transfer is temperature independent, in the framework of the Marcus theory[8] depicted in Fig. 5 the potential energy functions of the neutral (SP^*–BPL) and charged (SP^+–BPL^-) states should intersect at the minum of the SP^*–BPL potential. Any shift of the ionic state potential minimum, i.e. to higher as well as to lower values, induces a new crossing of the potential curves at activation barriers $\Delta E > 0$.

The quinone energy levels lie above all the chlorophyll and pheophytine energy levels. We attribute this to Coulomb repulsion with the net six negative charges on the H-unit of the photosynthetic reaction center. This interpretation is corroborated by the fact that a positively charged non-heme iron site shifts the quinone energy levels down. A neutralization of the six negative surface charges of the H-unit through H^+ is likely to lower considerably the quinone energy levels. In this respect it is interesting to note that the H-unit channels protons to the QB binding site, i.e. it is functionally favourable to have a high local concentration of protons near the H-unit.

The remaining ordering of energy levels of the functional branch chromophores BCLA and BPL is in accordance with the known features of primary electron transfer. The accessory chlorophyl (BCLA) energy level lies considerably above the pheophytine energy level. Considering the redox energy difference[9] $E_m(Chl) - E_m(Ph) \approx 5\frac{kcal}{mol}$ in identical solvents (Chlorophyll is more difficult to reduce than Pheophytine) the actual energy level of a reduced accessory Chlorophyll BCLA is not available for thermally assisted light-induced electron transfer.

3. Fluctuating and time-varying electrostatic energy

Because of the weak coupling between covalent and ionic states , i.e. SP^*–BPL and SP^+–BPL^-, compared with vibrational energies in the system, electron transfer

is possible only when covalent and ionic states are accidentally degenerate. This corresponds in the theory of Marcus[8] to a transition between covalent and ionic states only at crossings of potential energy surfaces (see Fig. 5). Due to Coulomb interactions with the surrounding protein matrix the energy difference between the covalent and ionic states fluctuates in accordance with thermal motions of the protein. The energy difference can also vary in time when the protein undergoes structural transitions, e.g. those induced by electron transfer between the chromophores. Obviously, the protein can regulate then through its motion the rate of electron transfer by controlling the coincidences of energy values of covalent and ionic states. We have investigated, therefore, how this energy difference for the primary electron transfer $\Delta E = E(\mathrm{SP^+}\text{–}\mathrm{BPL^-}) - E(\mathrm{SP^*}\text{–}\mathrm{BPL})$ varies during the simulated motion of a protein both before and after electron transfer. It should be pointed out, that electron transfer is controlled also by internal degrees of freedom, which can also be described by Marcus theory or by its quantum-mechanical generalizations.

In order to interprete the results of a molecular dynamics simulation regarding the energy $\Delta E(t)$ it is important to realize that **CHARMM** can only account for contributions to $\Delta E(t)$ due to interactions with charges outside the range of atoms which carry the positive and negative charge in the respective chromophores. Included in such calculations are neither the redox energy difference[9] which roughly measures $20\frac{kcal}{mol}$ for the SP*– BPL $\rightarrow$ $\mathrm{SP^+}$-$\mathrm{BPL^-}$– transfer, nor the Born energy relative to the polar solvents, e.g. DMF, in which redox energies are measured. Assuming a dielectric constant of $\epsilon \approx 2$ inside the protein, the Born energy for moving a single charge from DMF to the protein $\Delta E_B = \frac{e^2}{2r}(\epsilon^{-1} - \epsilon_{DMF}^{-1})$ for $r \approx 5\mathring{A}$ measures about $10\frac{kcal}{mol}$, twice that for two charges, and, hence, a total energy of about $40\frac{kcal}{mol}$ needs to be added to the pure external electrostatic contribution. This is, of course, a very rough estimate.

Uncertainties in the redox and Born energies don't allow to determine zero crossings of the energy difference between covalent and ionic states in proteins and, for that reason, we will present below in Fig. 6 only the electrostatic fraction of this energy difference. The electrostatic energy difference presented there has been calculated using **CHARMM**'s electrostatic energy function described above. The cut-off for this energy function is 9 Å. Also Coulomb interactions between nearest neighbours and next nearest neighbours in bonded systems were not included, as these energies were assumed to contribute to the redox energies. It must be emphasized here that the electrostatic potential of the previous section has been calculated differently, using Coulomb's law between all pairs of atoms in the X-ray protein structure, excluding only those atoms belonging to special groups of chromophore ring atoms. This latter type of calculation separates more clearly inter-molecular (electrostatic) from intra-molecular energy contributions in conjugated ring systems. It is therefore not surprising that both calculations yield quantitatively different results.

We calculated (**CHARMM**'s electrostatic) energy-differences both for a simulation before electron transfer and after the transfer. ΔE might also be interpreted as a measure for energy gain or loss due to electron forward or backward transport.

The result for the electrostatic energy difference $\Delta E(t)$ describing a transfer from the *special pair* to the pheophytine BPL is presented in Fig. 6 . The left part of the diagram shows ΔE before the transfer: it fluctuates around an energy value of about $-20\frac{kcal}{mol}$. This value corresponds to the equivalent value of $-27\frac{kcal}{mol}$ for the difference between the energy levels of $\mathrm{SP^+}$ and BPL in Fig. 2 (case ii). On the basis of a value of $40\frac{kcal}{mol}$ for the further contributions to the SP*–BPL and $\mathrm{SP^+}$–$\mathrm{BPL^-}$ energy difference one estimates an approximate energy of $-20 + 40 = 20\frac{kcal}{mol}$ for the excitation energy of the special pair.

It is suggestive to regard the crossings with the mean value $-20\frac{kcal}{mol}$ as the occurrences of energy degeneracies between the SP*–BPL and $\mathrm{SP^+}$–$\mathrm{BPL^-}$ energy levels. If this analogy holds , primary electron transfer is possible any time a crossing

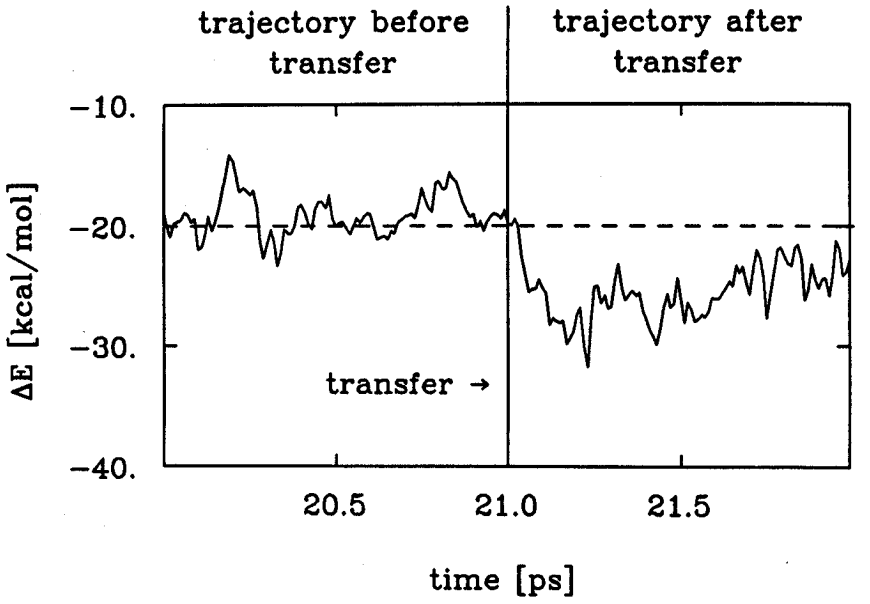

Fig. 6. Energy difference ΔE before and after electron transfer from special pair to BPL. The left part of the diagram displays ΔE obtained from molecular dynamics data (trajectory) before transfer. The instant the electron is transferred by changing the charge distribution on the special pair and BPL is denoted by an arrow. The right part shows ΔE after transfer obtained from molecular dynamics data (trajectory) after transfer.

occurs, i.e. 18 times in the case of Fig. 6. This behaviour demonstrates that protein fluctuations can control primary electron transfer. The situation that crossings with the mean value of $\Delta E(t)$ implies energy degeneracies in the Marcus theory corresponds to the case in this theory that the potential energy functions of the neutral (SP*–BPL) and charged (SP^+–BPL^-) states intersect at the **minum** of the SP*–BPL potential (see Fig. 5). Obviously, temperature lowering in this situation leads to more frequent crossings with the mean value and larger transfer rates, a behaviour observed for the reaction center.

We want to consider now how electron transfer affects $\Delta E(t)$ and, in particular, if back-transfer can be controlled (hindered) by protein relaxation and fluctuation. We have transferred, therefore, an electron in our simulations (by altering the chromophore charge distributions) at the instant marked by an arrow in Fig. 6 (at the time labeled 21 ps). $\Delta E(t)$ within 0.3 ps after the transfer decreases by about $10\frac{kcal}{mol}$ and then relaxes to a value close to $-25\frac{kcal}{mol}$. This is $5\frac{kcal}{mol}$ below the $-20\frac{kcal}{mol}$ value before transfer which at room temperature is just enough to prevent further crossings with the $-20\frac{kcal}{mol}$ line and, hence, back-transfer. It might be interesting to note that the very rapid initial relaxation appears to be very effective in preventing back-transfer already after about 100 fs. Furthermore, relaxations are sufficient to prevent back-transfer, however, do so with a minimal (exothermic) energy loss.

What processes contribute to the relaxation of $\Delta E(t)$ after electron transfer? Part of the relaxation will certainly be due to the motion of the pheophytine (BPL) ring towards the *special pair* which we discussed extensively in Ref. 3. Because of the large mass of the whole pheophytine ring moiety we expect that this motion will only participate in the slow component of the relaxation. The fast (.3 ps) decrease of $\Delta E(t)$ should be attributed to rearrangements of smaller dipolar side groups of the protein. To test this supposition we have monitored the electrostatic interaction of the tryptophane L100 which lies close to the BPL tetrapyrol ring and can form

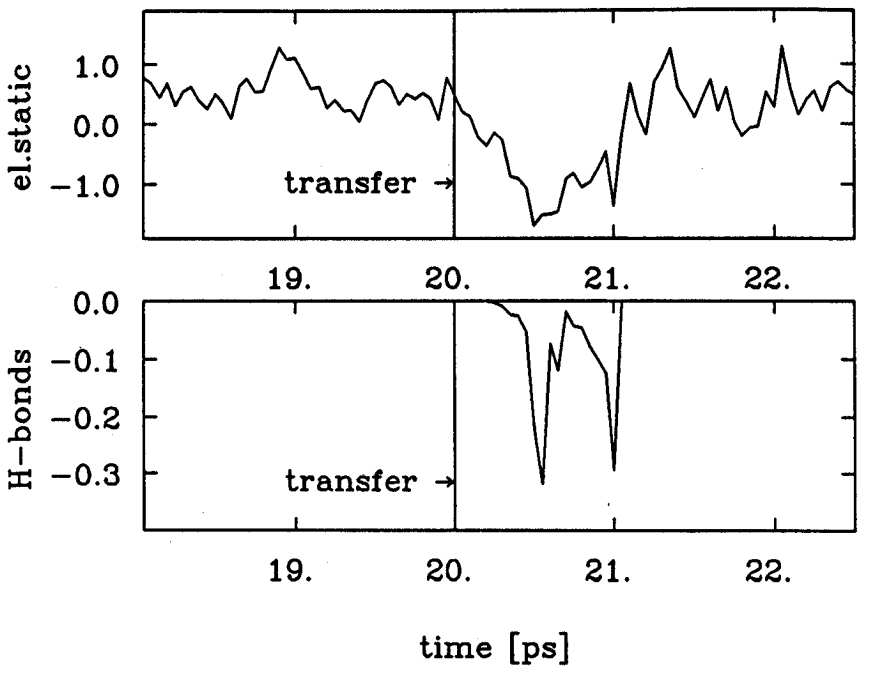

Fig. 7. Electrostatic and hydrogen-bond energy between BPL and a neighboring tryptophane residue (L100) before (time < 20 ps) and after (time > 20 ps) electron transfer to BPL. (Energies are given in $\frac{kcal}{mol}$*)*

a hydrogen bond with BPL. The behaviour of this group is illustrated in Fig. 7 through its time-dependent electrostatic interaction and through its hydrogen bonding behaviour. One observes that the electrostatic energy of this group decreases very rapidly after electron transfer. Also this group forms a transient hydrogen bond. Of course, this group contributes only a small fraction to $\Delta E(t)$.

Our results suggest that the protein after primary transfer stabilizes the electron to prevent back-transfer.

ACKNOWLEDGEMENTS

The authors like to thank A. Brünger, M. Karplus, Z. Schulten and P. Tavan for advice and help. This work has been supported by the Deutsche Forschungsgemeinschaft (SFB 143-C1) and by the National Center of Supercomputer Applications in Urbana, IL.

REFERENCES

1. J. Deisenhofer, O. Epp, K. Miki, R. Huber, H. Michel, X-ray Structure Analysis of a Membrane Protein Complex J molec Biol 180:385 (1984)
2. J. Deisenhofer, O. Epp, K. Miki, R. Huber, H. Michel, Structure of the protein subunits in the photosynthetic reaction center of Rhodopseudomonas viridis at 3 Å resolution, Nature 318:618 (1985)
3. H. Treutlein et al., Molecular dynamics simulation of the prim ary processes of the photosynthetic reaction center of Rps. viridis, contribution to this workshop

4. A. Warshel, S. T. Russel, Calculations of electrostatic interactions in biological systems and in solution, Q Rev Biophys 17:283 (1984)

5. I. Klapper et al., Focussing of electric fields in the active site of Cu-Zn superoxide dismutase: effects of ionic strength and amino-acid modification, Proteins 1:47 (1986)

6. B. R. Brooks et al. , CHARMM: A Program for Macromolecular Energy Minimization, and Dynamics Calculations, J Comp Chem 4:187 (1983)

7. T. O. Yeates et al., Structure of the reaction center from Rhodobacter sphaeroides R-26: Membrane-protein interactions, PNAS 84:6438 (1987)

8. R. A. Marcus, N. Sutin, Electron transfers in chemistry and biology, Biochim Biophys Acta 811:265 (1985)

9. Fajer et al., JACS 100:1918 (1978)